

The Nature of Ammonium and Methylammonium Halides in the Vapour Phase: Hydrogen Bonding *versus* Proton Transfer

A. C. Legon

Department of Chemistry, University of Exeter, Stocker Road, Exeter EX4 4QD

1 Introduction

A striking experience, common to most young chemists, is the veil of white fog that hangs eerily over the benches of a school laboratory after a period of vacant calm. The image is both enduring and thought provoking. When encountered in later life the phenomenon is redolent of chemistry in childhood. What is the smoke? Why and how is it formed?

The smoke consists, of course, of solid particles of ammonium chloride and has its origin in the slow interdiffusion of the vapours that leak from reagent bottles of '0.880' ammonia and 'conc.' hydrochloric acid. We learn somewhat later that each solid particle is composed of regular, interpenetrating arrays of ammonium (NH_4^+) and chloride (Cl^-) ions in a body-centred cubic lattice. Presumably, the separate vapours issuing from the two reagent bottles contain NH_3 and HCl molecules, respectively. This provokes further questions: How do NH_3 and HCl molecules interact to produce the ionic solid? What is the stable product of the interaction of a single NH_3 molecule and a single HCl molecule? Is it the simple hydrogen-bonded dimer $\text{H}_3\text{N}\cdots\text{HCl}$ or is a proton transferred from one to the other to give the ion pair $\text{H}_3\text{NH}^+\cdots\text{Cl}^-$? If the former, how does the ionic solid result? Are clusters $(\text{H}_3\text{N}\cdots\text{HCl})_m$ produced by further interactions of $\text{H}_3\text{N}\cdots\text{HCl}$ in the vapour until, eventually, the Coulombic stabilization associated with the ionic lattice facilitates proton transfers to give $(\text{H}_3\text{NH}^+\cdots\text{Cl}^-)_m$? At what value of m does this process occur? Are there analogues $\text{R}_{3-n}\text{H}_n\text{N}\cdots\text{HX}$ for which the ion pair $\text{R}_{3-n}\text{H}_n\text{NH}^+\cdots\text{X}^-$ is the most stable form in the dimer? What groups R and X and what values of n favour the ion pair?

The work described in this review was stimulated by such childhood memories and more mature reflection. Its aim was to answer some of the questions posed above. It was enabled by the development of a powerful tool: rotational spectroscopy of supersonically expanded jets. This technique allows the isolation and detailed characterization of dimers such as $(\text{NH}_3, \text{HCl})$ before clustering and precipitation can occur. Section 2 describes in outline the technique, the dimer properties to which it leads, and the special problems associated with its application to ammonium and methylammonium halides.

The results for the heterodimer $(\text{NH}_3, \text{HCl})$ in the vapour of

the archetypal substance ammonium chloride and their interpretation in the light of limiting hydrogen-bond $\text{H}_3\text{N}\cdots\text{HCl}$ and ion-pair $\text{H}_3\text{NH}^+\cdots\text{Cl}^-$ models are discussed in some detail in Section 3. The ways in which ammonium chloride might be modified to enhance ion-pair character in the heterodimer are explored in Section 4, wherein the conclusions available from analogous experiments conducted on carefully selected series of ammonium and methylammonium halides are also presented. The consistency of the experimentally derived conclusions of Section 4 with simple energetic arguments is examined in Section 5 while the consequences of replacing N by its second row analogue P are reviewed in Section 6.

2 How Can the Nature of Heterodimers ($\text{R}_{3-n}\text{H}_n\text{N}, \text{HX}$) in the Vapour Phase be Established Experimentally?

Much of our detailed knowledge of the geometry and electric charge distributions of simple molecules has been derived from spectroscopic constants gained by analysis of rotational spectra. But the application of rotational spectroscopy to heterodimers ($\text{R}_{3-n}\text{H}_n\text{N}, \text{HX}$) in the vapour of even the simplest members of the series, namely the ammonium and methylammonium halides, presents several problems which are discussed in 2.1 below. A form of spectroscopy that allows the problems to be overcome is outlined in 2.2 together with a summary of the spectroscopic constants and the molecular properties thereby available. The interpretation of spectroscopic constants to yield molecular properties requires limiting models for a hydrogen-bonded and an ion-pair heterodimer to be chosen. These are discussed in 2.3.

2.1 What Problems are Encountered in the Spectroscopy of Heterodimers ($\text{R}_{3-n}\text{H}_n\text{N}, \text{HX}$)?

Rotational spectroscopy is conducted on gases. The ammonium and methylammonium halides, which are the only members of the series ($\text{R}_{3-n}\text{H}_n\text{N}, \text{HX}$) so far investigated by rotational spectroscopy, have suitable vapour pressures at temperatures in the approximate range 200–300°C. Unfortunately, at such temperatures and pressures the vapour is almost completely dissociated into the amine and HX , with only a tiny fraction of the equilibrium mixture present as the heterodimer. Cooling the vapour will increase the mole fraction of heterodimer but decreases the vapour pressure at the same time. It is difficult to find a compromise temperature at which the number density of heterodimers is detectable. What is required is a method of cooling the mixture of amine and HX but without the concomitant precipitation of the solid ammonium halide. Such a method exists. It involves supersonic expansion of a dilute mixture of the component substances in, for example, argon through a pin hole into a vacuum to form a jet. The properties of supersonic expansions are well known.¹ Of most significance here are the efficient formation of the heterodimer by three-body collisions early in the expansion and the subsequent rapid onset of the collisionless phase of the expansion. Heterodimers surviving until the collisionless phase will then persist until they encounter a wall of the vacuum chamber. No further clustering or precipitation is possible and hence the molecules can be interrogated by microwave radiation at this stage to give their rotational spectra (see 2.2 below). Because of the very low effective temperature in

A. C. Legon is the Professor of Physical Chemistry in the University of Exeter. He was born at Rookery Farm, near Sudbury in Suffolk but was educated in London: at the Coopers' Company School, Bow and afterwards at University College London. His recent research interests include a systematic investigation of the nature of hydrogen-bonded dimers and other types of complex through the spectroscopy of supersonic jets. He was Tilden Lecturer and Medallist of the Royal Society of Chemistry for 1989–90.



the expanded gas, almost all heterodimer molecules are in their vibrational ground state

The mixture of the active components in argon can be achieved simply by entraining in argon the vapour in equilibrium with the heated salt.^{2,3} When X = Br or I, however, the hot vapour is very reactive and attacks the containing metal vessel. In such cases, a more satisfactory approach is to use the so-called fast-mixing technique.^{4,5} The components are then held separately at room temperature until the point at which they expand, simultaneously and coaxially, into the vacuum. Precipitation of the solid is again avoided and the resulting jet is rich in the heterodimer species of interest.

2.2 Rotational Spectroscopy of Supersonic Jets containing $(R_{3-n}H_nN, HX)$

The properties of the $(R_{3-n}H_nN, HX)$ heterodimers discussed here have been obtained from their rotational spectra observed by a technique called pulsed-nozzle, Fourier-transform microwave spectroscopy.^{6,7} A short pulse of the gas mixture of interest is expanded supersonically from a relatively high pressure through the nozzle (pin hole) into a vacuum. When the gas pulse is in collisionless expansion, it interacts with a pulse of microwave radiation. If the latter contains frequencies that coincide with a rotational transition of the heterodimer of interest, a macroscopic electric polarization is induced in the ensemble of molecules. Compared with the pulse of microwave radiation, the macroscopic polarization of the sample is long lived and therefore the spontaneous coherent radiation emitted when the polarization subsequently decays can be detected as a free induction decay in the time domain but in the absence of any background radiation. Fourier-transformation of these signals leads to the usual rotational spectrum in the frequency domain. The reader will be familiar with the pulsed NMR experiment in which a magnetic polarization is induced in an ensemble of nuclear spin vectors and the NMR transition is detected as a free induction decay. The microwave experiment outlined above is the exact electric analogue of the NMR experiment. The physics of the two methods is identical except that the polarization by microwave radiation involves the alignment of electric rather than magnetic dipoles and that the characteristic time of the free induction decay in the microwave region is much shorter.

In the present context, the essential feature of the pulsed-nozzle FT microwave spectrometer is the nozzle that produces the gas pulse. Two types of nozzle used here have been referred to above: the heated nozzle and the fast-mixing nozzle. Both are based on a solenoid valve which forms the gas pulse. In the heated nozzle, solid ammonium chloride (for example) is contained in a channel concentric with a 0.7 mm circular hole in a chamber attached to the base plate of the solenoid valve. The chamber is heated to a temperature at which the vapour pressure above the solid is sufficient. When the solenoid valve is activated, the 0.7 mm hole is opened and the vapour above the salt, entrained in a suitable quantity of argon, expands through it into the vacuum chamber of the spectrometer. In this way a supersonically expanded jet is produced. The timescale of the expansion is very short: the period between the equilibrium gas mixture entering the nozzle and the collisionless expansion phase in the vacuum chamber being only about 10 μ s. As a result, the extent of clustering is kept small and little solid is formed. The concentration of heterodimers (NH_3, HCl) in the expanded gas is, on the other hand, substantial.

The fast-mixing nozzle consists of the assembly illustrated in Figure 1. It is attached coaxially to the base plate of a solenoid valve.⁵ A pulse of gas mixture of (e.g.) 1% trimethylamine in argon from the solenoid valve passes through the outer of the two concentric tubes, as indicated by the arrow. Meanwhile, a mixture of (e.g.) 30% HBr in argon flows continuously through the inner tube (0.25 mm internal diameter). The two gas flows meet only as they expand into the vacuum chamber. At the boundary between the inner and outer components of the concentric flow which constitutes the jet, the heterodimer of

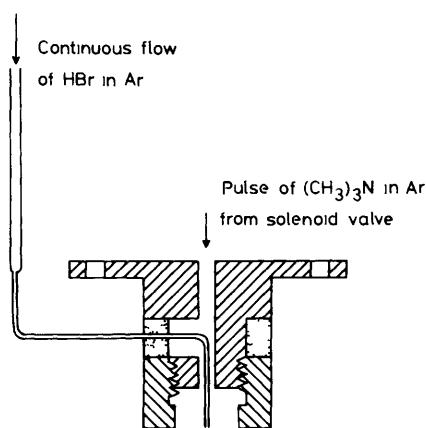


Figure 1 Fast mixing nozzle used to observe the rotational spectra of species such as $[(CH_3)_3N, HBr]$. The $(CH_3)_3N/Ar$ mixture is pulsed from a solenoid valve, onto the bottom of which the fast-mixing nozzle shown is attached. The continuous flow of HBr/Ar from the inner tube meets the pulse of gas from the outer tube in a concentric flow and $[(CH_3)_3N, HBr]$ is formed at the confluence without precipitation.

(e.g.) trimethylamine and HBr is formed in detectable quantity⁴ while precipitation of the solid is again minimal.

2.3 Spectroscopic Constants and their Interpretation: Limiting Models

Once observed by the above-described technique, the ground-state rotational spectra of heterodimers in the series $(R_{3-n}H_nN, HX)$ can be analysed to give a variety of spectroscopic constants. These constants can be interpreted in turn to give the dimer properties and the nature of the intermolecular interaction. This observation gives an immediate insight into the heterodimer geometry – it must have at least C_3 symmetry. The rotational constants B_0 determined from analyses of such spectra are the ground-state values and are related to the distribution of mass (moment of inertia) in the vibrationless state in a complicated, but well understood, manner. It is customary to use B_0 values as though they were equilibrium values (the differences are relatively small) to obtain bond lengths and angles (the so-called r_0 and r_s -values). Following this convention, B_0 values and their changes on isotopic substitution can be interpreted in terms of the separation of the $(CH_3)_{3-n}H_nN$ and HX subunits in the heterodimer, if unperturbed monomer geometries are assumed. All bond lengths considered here are of the r_0 -type.

Table 1 sets out the spectroscopic phenomena/constants of principal interest in connection with this discussion of the ammonium and methylammonium halides and indicates the heterodimer properties to which they lead. The final column of Table 1 gives some comments about models used. All but one of the heterodimers considered here exhibit symmetric-top type rotational spectra. This observation gives an immediate insight into the heterodimer geometry – it must have at least C_3 symmetry. The rotational constants B_0 determined from analyses of such spectra are the ground-state values and are related to the distribution of mass (moment of inertia) in the vibrationless state in a complicated, but well understood, manner. It is customary to use B_0 values as though they were equilibrium values (the differences are relatively small) to obtain bond lengths and angles (the so-called r_0 and r_s -values). Following this convention, B_0 values and their changes on isotopic substitution can be interpreted in terms of the separation of the $(CH_3)_{3-n}H_nN$ and HX subunits in the heterodimer, if unperturbed monomer geometries are assumed. All bond lengths considered here are of the r_0 -type.

The centrifugal distortion constant D_J of a symmetric-top heterodimer, which allows for the slight dependence of the molecular geometry on rotational state ignored in the rigid rotor limit, can be interpreted in terms of one measure of the strength of intermolecular binding by using a simple model. The monomers are assumed rigid and unchanged in geometry on dimer formation. The constant D_J depends in the quadratic approximation on only the intermolecular stretching force constant k_r according to⁸

$$k_r = (16 \pi^2 B_0^3 \mu / D_J)(1 - B_0 / B_{Base} - B_0 / B_{HX}) \quad (1)$$

Table 1 Spectroscopic constants, properties and limiting models of heterodimers [(CH₃)_{3-n}H_nNHX] from rotational spectroscopy

Spectroscopic property	Heterodimer property	Limiting model
(1) Form of spectrum	Symmetry	Symmetric top ($A > B = C$) Asymmetric top ($A > B > C$) Semi-rigid rotor in either hydrogen-bond (CH ₃) _{3-n} H _n N...HCl or ion-pair (CH ₃) _{3-n} H _n NH ⁺ ...X limit
(2) Rotational constants A_0, B_0, C_0	Radial and angular geometry $r(\text{N}\cdots\text{X})$ and relative orientation of components	Unchanged monomer geometries assumed, orientation (where appropriate) of subunits fitted
(3) Centrifugal distortion constant D_J	Intermolecular stretching force constant k_σ	(a) Simple hydrogen-bond model, ^a $e g$ HCN...HCl, $k_\sigma = 9.12 \text{ Nm}^{-1}$ (b) Ion pair model ^b $e g$ Na ⁺ ...Cl ⁻ , $k_\sigma = 108.6 \text{ Nm}^{-1}$
(4) X or ¹⁴ N nuclear quadrupole coupling constants $\chi(X)$ or $\chi(^{14}\text{N})$	Electric field gradient along principal inertial axis at X or ¹⁴ N	(a) Simple hydrogen bond model, ^a $e g$ HCN...HCl, $\chi(^{35}\text{Cl}) = -53.720(2) \text{ MHz}$ (b) Ion-pair model, ^b $e g$ Na ⁺ ...Cl ⁻ , $\chi(^{35}\text{Cl}) = -5.643(4) \text{ MHz}$

A C Legon, E J Campbell and W H Flygare *J Chem Phys* 1982 76 2267 and Ref 11. ^b Calculated using $\omega_e = (2\pi c)^{-1}(k/\mu)^{1/2}$ from P L Clouser and W Gordy *Phys Rev A* 1964 134 A863. F H de Leeuw, R Van Wachem and A Dymanus Symposium on Molecular Structure and Spectroscopy Ohio 1969 Abstract R5

where $\mu = m_{\text{Base}}m_{\text{HX}}/(m_{\text{Base}} + m_{\text{HX}})$ and $B_0, B_{\text{Base}}, B_{\text{HX}}$ are zero-point rotational constants of the heterodimer, the base, and the acid HX, respectively. k_σ is the restoring force per unit infinitesimal extension of the intermolecular bond and is a measure of the energy required for unit infinitesimal extension. It is an important quantity here, for it changes by an order of magnitude between a typical hydrogen-bonded heterodimer ($e g$ HCN...HCl) and a typical ion pair ($e g$ Na⁺...Cl⁻) (see Table 1). The variation of k_σ along selected series [(CH₃)_{3-n}H_nNHX], to be discussed below, provides a criterion of hydrogen-bond/ion-pair character.

The spectroscopic quantities/phenomena that are perhaps most revealing of the nature of [(CH₃)_{3-n}H_nNHX] in the vapour are the halogen and ¹⁴N-nuclear quadrupole coupling constants and the Stark effect. The latter is the splitting induced in rotational transitions by a uniform applied electric field and can be analysed to give the electric dipole moment of the molecule. This effect will not be used here. Nuclear quadrupole hyperfine structure in rotational transitions arises from the coupling of a nuclear spin vector I with the rotational angular momentum vector J through the interaction of the electric quadrupole moment Q of the nucleus in question with the electric field gradient at that nucleus. The number of discrete relative orientations of I and J is limited to that group for which the magnitude of the resultant $I + J = F$ is given by $\{F(F+1)h^2\}^{1/2}$, where

$$F = I + J, I + J - 1, \dots, |I - J| \quad (2)$$

Each orientation corresponds to a slightly different potential energy of interaction of Q with the electric field gradient and

hence each rotational energy level, labelled by J , is split into $2I + 1$ components (if $J > I$), labelled by F . Rotational transitions exhibit a corresponding hyperfine structure, the pattern being determined by the F and J selection rules. For a symmetric top molecule carrying on its axis a quadrupolar nucleus X, the associated observable spectroscopic quantity is the nuclear quadrupole coupling constant $\chi(X)$. This is linearly related to the electric field gradient $V_{zz} = -\partial^2 V/\partial z^2$ at X along the molecular symmetry axis z by

$$\chi(X) = -eV_{zz}Q \quad (3)$$

where e is the magnitude of the protonic charge. As $\chi(X)$ increases, the hyperfine splitting in a given transition increases. Since V_{zz} at X arises from the particular distribution of electrons and nuclei in the molecule, the quadrupolar nucleus, through equation 3, provides a probe of the electric charge distribution in the molecule, once $\chi(X)$ is known.

Limiting values of $\chi(X)$ in the free monomers and in molecules chosen to model simple hydrogen-bonded and ion-pair heterodimers will be important in what follows. As an example, $\chi(^{35}\text{Cl})$ will be considered⁹ but similar arguments apply to ¹⁴N, Br, and I nuclei and will be used later. An isolated ³⁵Cl⁻ ion with the electronic configuration [K L 3s²3p⁶] is spherically symmetric and therefore $V_{zz} = 0$ and $\chi(^{35}\text{Cl}) = 0$. An isolated atom ³⁵Cl[K L 3s²3p⁵] is generated when an electron is removed from a 3p orbital and the resulting V_{zz} leads to $\chi(^{35}\text{Cl}) = -109.74 \text{ MHz}$. It is convenient to describe an isolated hydrogen chloride molecule through the valence-bond structures H-Cl and H⁺Cl⁻. The former has a 3p² electron deficiency, like the Cl atom, while the latter has $\chi(^{35}\text{Cl}) = 0$. The observed value¹⁰ $\chi(^{35}\text{Cl}) = -67.62 \text{ MHz}$ for gaseous HCl can then be readily understood through weighting the contributions of the valence bond structures. When an axially symmetric molecule, like HCN, is brought up to HCl along the z -axis to form a simple hydrogen-bonded dimer HCN...HCl (no proton transfer), $\chi(^{35}\text{Cl})$ changes slightly (see Table 1) because of the changed electric field gradient at Cl due to the HCN electric charge distribution and because of the additional zero-point motion available to HCl in the dimer. These contributions to $\chi(^{35}\text{Cl})$ have been modelled (see Section 3.2 below).

If the heterodimer (CH₃)_{3-n}H_nNH⁺...Cl⁻ were an ion pair, it could be viewed as arising when the appropriate methylammonium ion is brought up to an isolated Cl⁻ ion. The quantity $\chi(^{35}\text{Cl}) = 0$ appropriate to Cl⁻ in isolation then increases somewhat in magnitude as a result of the distortion of the spherically symmetric charge distribution of the anion by the cation. A suitable model for such an ion pair is an alkali chloride diatomic molecule in the gas phase. For example, $\chi(^{35}\text{Cl})$ is only $-5.643(4) \text{ MHz}$ in Na⁺...Cl⁻ (See Table 1).

3 The Heterodimer (NH₃, HCl): A Case Study

The ground-state rotational spectra of the most abundant isotopomer (¹⁴NH₃, H³⁵Cl) of the ammonia-hydrogen chloride dimer and those obtained by single isotopic substitution at each different atom have been measured in the vapour above solid ammonium chloride.^{2,3} The heated nozzle discussed above was used in the pulsed-nozzle FT microwave spectrometer in this case. The set of spectroscopic constants determined from the spectra are recorded in Table 2. They can be interpreted, first qualitatively and then quantitatively, to establish the nature of the heterodimer (NH₃, HCl) in the gas phase.

3.1 Qualitative Interpretation of Spectroscopic Constants

The rotational spectrum of (NH₃, HCl) is of the symmetric-top type. The only way in which HCl can be bound to NH₃ to achieve this result is in a heterodimer of C_{3v} symmetry. Moreover, the only geometry of this symmetry that is consistent with the observed changes in the rotational constant B_0 (which is proportional to the moment of inertia I_b through $B_0 = h/8\pi^2 I_b$)

Table 2 Observed ground-state spectroscopic constants of isotopomers of (NH₃,HCl) in ammonium chloride vapour.^a

Isotopomer	B_0 /MHz	D_J /kHz	D_{JK} /kHz	$\chi(\text{Cl})$ /MHz	$\chi(^{14}\text{N})$ /MHz
(¹⁴ NH ₃ ,H ³⁵ Cl)	4243.2593(16)	12.8(2)	371.5(8)	-47.607(9)	-3.248(14)
(¹⁵ NH ₃ ,H ³⁵ Cl)	4098.3113(12)	11.6(2)	344.2(5)	-47.614(5)	—
(¹⁴ NH ₂ D,H ³⁵ Cl) ^b	4033.8388(16)	11.4(2)	—	-47.481(9)	-3.312(16)
(¹⁴ NH ₃ ,D ³⁵ Cl)	4228.932(1)	12.6 ^c	—	-48.630(16)	-3.27(2)
(¹⁴ NH ₃ ,H ³⁷ Cl)	4168.8107(9)	12.0(1)	357.7(6)	-37.531(6)	-3.264(10)

^a From Ref. 3. ^b Asymmetric rotor species. Value in B_0 column is $(B_0 + C_0)/2$. ^c Assumed value, see Ref. 3 for justification.

is the one³ in which the nuclei lie in the order H₃N⋯HCl. But the position of the hydrogen-bond proton along the C_{3v} axis in the equilibrium geometry is uncertain and each of the three models of C_{3v} symmetry shown in Figure 2 is consistent with the observed rotational constants. The reason for the uncertainty in the position of this proton lies in its proximity to the dimer centre of mass. Then D-substitution leads to only a small change ΔI_b^D in the equilibrium moment of inertia while the change in the zero-point motion attending this substitution tends to make ΔI_b smaller than ΔI_b^D . In any case, ΔI_b^D depends on z_H^2 and hence we cannot tell on which side of the centre of mass the proton lies. How then can we discriminate between the three models (ion-pair, intermediate-type, and hydrogen-bonded) shown in Figure 2?

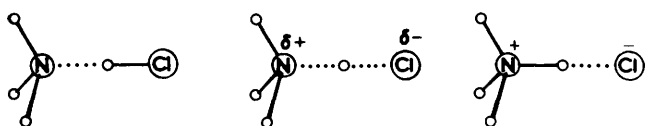


Figure 2 Three possible structures of C_{3v} symmetry for the (NH₃,HCl) dimer in which the nuclei lie in the order H₃N⋯HCl; namely, the hydrogen-bonded form, a form with partial proton transfer, and a form with complete proton transfer.

A qualitative distinction is immediately possible from the magnitudes of $\chi(^{35}\text{Cl})$ and k_σ (as determined from D_J by the method outlined in Section 2.3). Table 3 lists $\chi(^{35}\text{Cl})$ and k_σ for H₃N⋯HCl and a selection of model systems, namely the isolated HCl molecule, a typical hydrogen-bonded dimer HCN⋯HCl, and a typical ion pair Na⁺⋯Cl⁻. For H₃N⋯HCl, each of these quantities is closer to the corresponding value for HCN⋯HCl than that of Na⁺⋯Cl⁻. Qualitatively, at least, we conclude that the simple hydrogen-bonded model H₃N⋯HCl is more appropriate. Are the numerical values of $\chi(^{35}\text{Cl})$ and k_σ also quantitatively consistent with this model?

3.2 Quantitative Interpretation of $\chi(^{35}\text{Cl})$ and k_σ

It can be shown that both $\chi(^{35}\text{Cl})$ and k_σ are quantitatively as expected for the hydrogen-bonded model H₃N⋯HCl.

Table 3 Comparison of Cl nuclear quadrupole coupling constants $\chi(\text{Cl})$ and intermolecular stretching force constants k_σ of (NH₃,HCl) and various model systems

Molecule	Reason for choice	$\chi(^{35}\text{Cl})$ /MHz	k_σ /Nm ⁻¹
HCl	Isolated component	-67.6189 ^a	—
HC ¹⁴ N⋯HCl	Hydrogen-bond model	-53.720(2) ^b	9.12 ^b
(¹⁴ NH ₃ ,HCl)	Test	-47.607(9) ^c	17.6(3) ^c
Na ⁺ ⋯Cl ⁻	Ion-pair model	-5.643(4) ^d	108.6 ^e
Cl ⁻	Free anion	0.0	—

^a Ref. 10. ^b See footnote a of Table 1. ^c Ref. 3. ^d See footnote c of Table 1. ^e See footnote b of Table 1.

A consideration of the k_σ for an extended series of heterodimers B⋯HX has revealed that the experimental values can be reproduced by a simple empirical equation

$$k_\sigma = c E N \quad (4)$$

where $c = 0.25 \text{ Nm}^{-1}$ and E and N are numerical electrophilicities and nucleophilicities assigned to the donor region of HX and the acceptor region of B, respectively.¹¹ If E for HF is chosen as 10, equation 4 gives the set of N values for the series of B indicated in Figure 3 by using the k_σ of the corresponding B⋯HF. The plot of k_σ versus N for the series B⋯HF is then by definition a straight line. When k_σ for the analogous series B⋯HCl is plotted against the same N values (also in Figure 3), the result is also a straight line through the origin. In this case, we note that the point for H₃N⋯HCl lies on the straight line. Thus, k_σ for H₃N⋯HCl is well behaved and has the value expected by extrapolation from the more weakly bound members of the series. But it can be shown that in the series B⋯HF there is only tiny HF bond lengthening on dimer^{12,13} formation. Hence, it appears that the above arguments indicate only negligible extension of HCl and therefore no significant extent of proton transfer in H₃N⋯HCl. On the other hand, while k_σ for (CH₃)₃N⋯HF lies on its straight line^{13,14} in Figure 3, that of (CH₃)₃N⋯HCl certainly does not¹⁵ (see Section 4.2).

To show that $\chi(^{35}\text{Cl})$ for H₃N⋯HCl is quantitatively predicted by using the simple hydrogen-bonded model of the dimer,

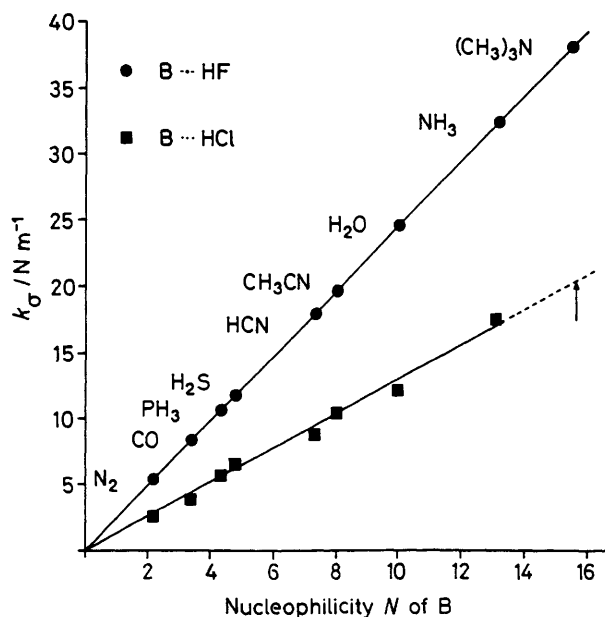


Figure 3 Systematic relationship between the intermolecular stretching force constant k_σ of dimers B⋯HF and B⋯HCl and the nucleophilicity N of the donor region of B (see text for discussion). The N values of B are chosen so that the k_σ for B⋯HF lie on a straight line. The k_σ for B⋯HCl are then also a linear function of the N values. The extrapolated value of k_σ for the hydrogen-bonded model of (CH₃)₃N⋯HCl is indicated by the arrow.

we must calculate the change $\Delta V_{zz}^{\text{Cl}}$ in the electric field gradient at Cl when NH_3 is brought up from infinite distance to its equilibrium position along z . We consider first the equilibrium (vibrationless) C_{3v} geometry. The expression for $\Delta V_{zz}^{\text{Cl}}$ is then¹⁶

$$\Delta V_{zz}^{\text{Cl}} = g_{zz,z}^{\text{Cl}} F_z + (1 + \frac{3}{2} g_{zz,zz}^{\text{Cl}}) F_{zz} + \frac{5}{2} g_{zz,zzz}^{\text{Cl}} F_{zzz} + \dots \\ \dots + \frac{1}{2} \epsilon_{zz,zz}^{\text{Cl}} F_z^2 + \dots \quad (5)$$

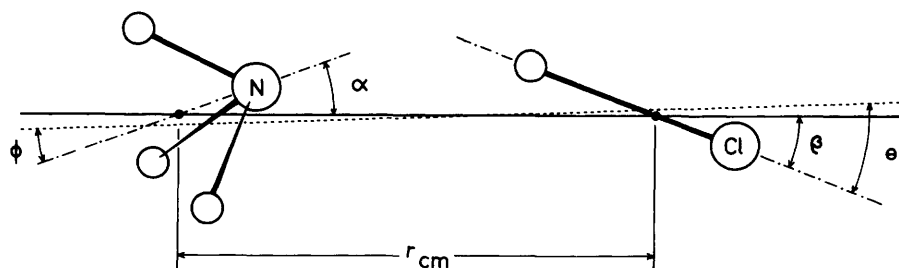
In equation 5, F_z , F_{zz} , *etc.* are the electric field, the gradient of the electric field, *etc.* due to NH_3 but at the position along the symmetry axis z occupied by the Cl nucleus. (The convention V_{zz} for an intrinsic field gradient and F_{zz} for that external to a group of charges is in use.) The terms $g_{zz,z}^{\text{Cl}}$, $g_{zz,zz}^{\text{Cl}}$, *etc.* are the axial components of the HCl response tensors. Thus $g_{zz,z}^{\text{Cl}}$ is the electric field gradient at Cl along z induced by a unit external electric field. $g_{zz,zz}^{\text{Cl}}$ measures the additional electric field gradient induced at Cl in response to a unit electric field gradient along z , and so on. These g -tensor components have been calculated *ab initio* for HCl by Baker *et al.*¹⁶ The values of F_z , F_{zz} , *etc.* have been estimated at the appropriate distance (see Section 3.3 below) from NH_3 along z by Fowler¹⁷ using a distributed multipole analysis to represent the electric charge distribution of NH_3 . Application of equation 5 then leads to a value of $\Delta V_{zz}^{\text{Cl}}$ which corresponds to a correction $\Delta \chi_e(^{35}\text{Cl}) = -e \Delta V_{zz}^{\text{Cl}} Q \approx 13$ MHz to the free HCl coupling constant $\chi_0(^{35}\text{Cl}) = -67.62$ MHz. Hence, the *equilibrium* Cl-nuclear quadrupole coupling constant for the hydrogen-bonded model of $\text{H}_3\text{N} \cdots \text{HCl}$ is predicted to be $\chi_e(^{35}\text{Cl}) \approx -55$ MHz, which is close to the observed ground-state value $\chi(^{35}\text{Cl}) = -47.607(9)$ MHz.

Even closer agreement between the model value $\chi_e(^{35}\text{Cl})$ and the experimental value $\chi(^{35}\text{Cl})$ is obtained when the effects of zero-point averaging are added to the model. The value of the Cl-nuclear quadrupole coupling constant in the zero-point state is given according to the model by

$$\chi(^{35}\text{Cl}) = -eQ \langle V_{aa}^{\text{Cl}} + \Delta V_{aa}^{\text{Cl}} \rangle \quad (6)$$

where V_{aa}^{Cl} and $\Delta V_{aa}^{\text{Cl}}$ are now the instantaneous values of the electric field gradient at Cl along the a -axis of the dimer appropriate to unperturbed HCl and induced by NH_3 , respectively. The average is over the zero-point motion of $\text{H}_3\text{N} \cdots \text{HCl}$. The first term in equation 6 is simply $\langle V_{aa}^{\text{Cl}} \rangle = \frac{1}{2} \langle 3 \cos^2 \theta - 1 \rangle V_{zz}^{\text{Cl}} = \langle P_2(\cos \theta) \rangle V_{zz}^{\text{Cl}}$, where θ is the angle between the HCl direction and the instantaneous a -axis. The second term is much more complicated, as can be appreciated by examining the model for the zero-point motion of the dimer shown in Figure 4. The distance between the subunit mass centres is assumed fixed while the rigid subunits execute angular oscillations ϕ and θ defined with reference to the instantaneous a -axis. Clearly, the NH_3 oscillation ϕ affects F_z , F_{zz} , *etc.*, while each g -tensor term contributing to $\Delta V_{aa}^{\text{Cl}}$ has an appropriate coefficient $\langle P_n(\cos \theta) \rangle$. In the absence of the detailed term by term corrections, it is an acceptable approximation to assume that $\langle \Delta V_{aa}^{\text{Cl}} \rangle \approx \langle P_2(\cos \theta) \rangle \Delta V_{zz}^{\text{Cl}}$, where $\Delta V_{zz}^{\text{Cl}}$ is the equilibrium value. A detailed discussion³ indicates that $\cos^{-1} \langle \cos^2 \theta \rangle^{\frac{1}{2}} \approx 15^\circ$ is reasonable for $\text{H}_3\text{N} \cdots \text{HCl}$ and hence equation 6 leads to the prediction of

Figure 4 Definition of the angles ϕ , θ , α , β , and the distance r_{cm} used to discuss the geometry and the interpretation of the nuclear quadrupole coupling constants of $(\text{NH}_3, \text{HCl})$.



$\chi(^{35}\text{Cl}) \approx -49$ MHz for the simple hydrogen-bonded model of $\text{H}_3\text{N} \cdots \text{HCl}$. This value is close enough to the observed ground-state quantity to give confidence that the hydrogen-bonded model is quantitatively capable of accounting for the experimental value of $\chi(^{35}\text{Cl})$.

Similar arguments to those above could be made to show that the decrease in magnitude of $\chi_0(^{14}\text{N}) = -4.090$ MHz in free $^{14}\text{NH}_3$ to $\chi(^{14}\text{N}) = -3.248(14)$ MHz in $\text{H}_3^{14}\text{N} \cdots \text{HCl}$ (see Table 2) is also consistent with the simple hydrogen-bonded model.³ Unfortunately, however, the response tensor components $g_{zz,z}^{\text{NH}_3}$, *etc.*, are not available and quantitative comparison is not yet possible.

3.3 The Geometry of $\text{H}_3\text{N} \cdots \text{HCl}$

The arguments in Sections 3.1 and 3.2 establish that the heterodimer in ammonium chloride vapour is a simple hydrogen-bonded molecule $\text{H}_3\text{N} \cdots \text{HCl}$ of C_{3v} symmetry. In particular, it is unnecessary in interpreting the various spectroscopic constants to invoke any significant extent of proton transfer from HCl to NH_3 . These conclusions are consistent with matrix isolation studies¹⁸ and recent *ab initio* calculations.¹⁹

Having established the angular geometry $\text{H}_3\text{N} \cdots \text{HCl}$, the radial geometry is available from the B_0 values under the assumption that the geometries of NH_3 and HCl survive dimer formation. The model used (see Figure 4) attempts to account for the contribution of the intermolecular bending modes to the zero-point motion by allowing the NH_3 and HCl subunits to execute the angular oscillations α and β about their respective mass centres, the distance between which is fixed. It is readily shown that

$$\langle I_{bb} \rangle = \mu \langle r_{\text{cm}}^2 \rangle + \frac{1}{2} I_b^{\text{NH}_3} (1 + \langle \cos^2 \alpha \rangle) + \frac{1}{2} I_b^{\text{HCl}} \langle \sin^2 \alpha \rangle \\ + \frac{1}{2} I_b^{\text{HCl}} (1 + \langle \cos^2 \beta \rangle) \quad (7)$$

where r_{cm} , α , and β are defined in Figure 4 and $I_b^{\text{NH}_3}$ and I_b^{HCl} refer to the free monomers. In the approximation that the observed quantity for the heterodimer $I_b = h/8\pi^2 B_0$ can be used in place of $\langle I_{bb} \rangle$, equation 7 provides a route to $\langle r_{\text{cm}}^2 \rangle^{\frac{1}{2}}$. To a high degree of approximation $\langle \cos^2 \alpha \rangle$ and $\langle \cos^2 \beta \rangle$ can be taken as equal to $\langle \cos^2 \phi \rangle$ and $\langle \cos^2 \theta \rangle$, respectively, and the last two quantities have been established from $\chi(^{14}\text{N})$ and $\chi(^{35}\text{Cl})$, respectively. The values of $\langle r_{\text{cm}}^2 \rangle^{\frac{1}{2}}$ for each of the symmetric-top isotopomers are recorded in Table 4. Once $\langle r_{\text{cm}}^2 \rangle^{\frac{1}{2}}$ is available, the known geometries of NH_3 and HCl allow $r(\text{N} \cdots \text{Cl})$ to be calculated³ and these too are given in Table 4. The modelling of $\chi(^{35}\text{Cl})$ discussed in Section 3.2 employed the radial geometry displayed in Table 4.

4 Does Proton Transfer Occur in Gas-phase Ammonium or Methylammonium Halides?

The conclusion of Section 3 is unambiguous. The lowest energy form of the heterodimer in the vapour of the prototype ammonium halide has the simple hydrogen-bonded structure $\text{H}_3\text{N} \cdots \text{HCl}$. Furthermore, no evidence was found for an ion-pair form $\text{H}_3\text{NH}^+ \cdots \text{Cl}^-$ existing at a minimum of comparable potential energy. This raises an important question: Is it possible to modify $\text{H}_3\text{N} \cdots \text{HCl}$ chemically so that the ion-pair becomes the more stable, and possibly the only, form? A chemist would

Table 4 $\langle r_{\text{cm}}^2 \rangle^{\frac{1}{2}}$ and $r(\text{N}\cdots\text{Cl})$ for symmetric-top isotopomers of $\text{H}_3\text{N}\cdots\text{HCl}^a$

Isotopomer	$\langle r_{\text{cm}}^2 \rangle^{\frac{1}{2}}/\text{\AA}$	$r(\text{N}\cdots\text{Cl})/\text{\AA}$
$\text{H}_3^{14}\text{N}\cdots\text{H}^{35}\text{Cl}$	3 1654(2)	3 1364(7)
$\text{H}_3^{15}\text{N}\cdots\text{H}^{35}\text{Cl}$	3 1614(2)	3 1358(7)
$\text{H}_3^{14}\text{N}\cdots\text{D}^{35}\text{Cl}$	3 1367(2)	3 1410(11)
$\text{H}_3^{14}\text{N}\cdots\text{H}^{37}\text{Cl}$	3 1673(2)	3 1363(6)

^a For a detailed discussion of the values of $\langle \cos^2\alpha \rangle$ and $\langle \cos^2\beta \rangle$ used with equation 7 to evaluate these distances, see Ref 3. The errors in $\langle r_{\text{cm}}^2 \rangle^{\frac{1}{2}}$ and $r(\text{N}\cdots\text{Cl})$ are those arising from the assumed error of $\pm 3^\circ$ in $\alpha_{\text{av}} = \cos^{-1}\langle \cos^2\alpha \rangle^{\frac{1}{2}} = 15^\circ$

attempt to answer this question by reference to the group of ammonium and methylammonium halides in Figure 5

It is known that the energy required to dissociate HX into H^+ and X^- in the gas phase decreases along the series $\text{X} = \text{F}, \text{Cl}, \text{Br}, \text{I}$. Hence, the proton is more likely to be transferred from HX to $(\text{CH}_3)_{3-n}\text{H}_n\text{N}$ as we move down a vertical column of Figure 5. On the other hand, the gas-phase proton affinity of ammonia is increased progressively with the stepwise methylation of the base. Proton transfer might therefore be encouraged progressively along the horizontal series $(\text{CH}_3)_{3-n}\text{H}_n\text{N}\cdots\text{HCl}$ as n decreases from 3 to 0. The bottom right-hand corner of Figure 5 therefore favours ion-pair structures while the top left should lead to hydrogen-bonded dimers

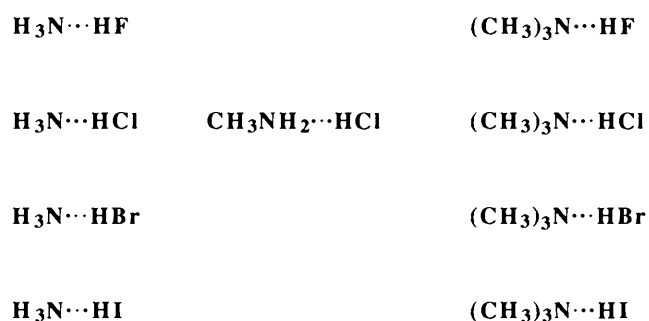


Figure 5 Series of dimers $(\text{CH}_3)_{3-n}\text{H}_n\text{N}\cdots\text{HX}$ investigated by rotational spectroscopy. In the left-hand vertical series, the proton affinity of the base NH_3 is fixed while the ease of dissociation of the hydrogen halide increases from F to I. In the central horizontal series, the proton affinity of the base increases progressively from left to right, while in the right-hand vertical series the proton affinity of the base is constant but has its maximum value

All of the heterodimers identified in Figure 5 have been investigated through their rotational spectra, all but one by the pulsed-nozzle FT technique. By consideration of the spectro-

scopic and molecular properties thereby available, especially $\chi(\text{X})$ and k_σ , which featured predominantly in the discussion of ammonium chloride, the question asked above can be answered. It is convenient first to consider the left-hand vertical series in Figure 5 to test the effect of weakening the HX bond while leaving the proton affinity of the base unchanged. The horizontal series $(\text{CH}_3)_{3-n}\text{H}_n\text{N}\cdots\text{HCl}$ ($n = 3, 2, 0$) then allows the effect of methylation of ammonia to be investigated for a fixed HX . Finally, the right-hand vertical series illustrates the effect of weakening the HX bond when the proton affinity of the base is maximized.

In the discussion that follows, we must bear in mind that spectroscopic techniques employing supersonic jets tend to detect only the vibrational ground-state of the lowest energy conformer of a molecule. Hence, the conclusions drawn below pertain to the lowest temperature form of $(\text{CH}_3)_{3-n}\text{H}_n\text{N}\cdots\text{HX}$. We cannot rule out a higher energy minimum on the potential surface since this would probably be depopulated in the expansion. As we shall see, however, there are reasons for believing that in general only one stable form (*either* hydrogen-bonded or ion pair) exists.

4.1 The Series $\text{H}_3\text{N}\cdots\text{HX}$ ($\text{X} = \text{Cl}, \text{Br}, \text{I}$)

The ground-state rotational spectrum of each member of the series $\text{H}_3\text{N}\cdots\text{HX}$ ($\text{X} = \text{Cl}, \text{Br}, \text{I}$) has been observed by the pulsed-nozzle FT microwave method and spectroscopic constants determined.^{3, 20, 21} Again, we focus attention on the critical quantities $\chi(\text{X})$ and k_σ , listed in Table 5, as the means to establish the nature of the lowest energy forms of the heterodimers. Also given in Table 5 are the corresponding quantities for free HX , for $\text{HCN}\cdots\text{HX}$ (the limiting hydrogen-bond model) and for $\text{Na}^+\cdots\text{X}^-$ (the limiting ion-pair model).

It is immediately evident that $\chi(\text{X})$ and k_σ are much closer in magnitude to their respective values in $\text{HCN}\cdots\text{HX}$ than in $\text{Na}^+\cdots\text{X}^-$. We note also that the ratio $\chi(\text{X})/\chi_{\text{HB}}(\text{X})$ is almost constant across the series $\text{X} = \text{Cl}, \text{Br}, \text{I}$, as is the ratio $k_\sigma/k_\sigma^{\text{HB}}$. Although a quantitative prediction of $\chi(^{35}\text{Cl})$ for the hydrogen-bonded model of $\text{H}_3\text{N}\cdots\text{HCl}$ was possible and gave good agreement with the observed value (see Section 3.2) such an approach is not possible for $\text{X} = \text{Br}$ or I because the required response tensor components g_{zzz}^{X} are not available for HBr and HI . Nevertheless, in view of the result for $\text{H}_3\text{N}\cdots\text{HCl}$ and the constancy of the ratios $\chi(\text{X})/\chi_{\text{HB}}(\text{X})$ and $k_\sigma/k_\sigma^{\text{HB}}$ it is very likely that both $\text{H}_3\text{N}\cdots\text{HBr}$ and $\text{H}_3\text{N}\cdots\text{HI}$ are simple hydrogen-bonded dimers. $\text{H}_3\text{N}\cdots\text{HF}$ has been investigated using the molecular beam electric resonance technique.²² The D_J value leads, *via* equation 1, to $k_\sigma = 32.8 \text{ Nm}^{-1}$ which compares with the limiting values^{8, 23} of 18.2 and 176.1 Nm^{-1} for $\text{HCN}\cdots\text{HF}$ and $\text{Na}^+\cdots\text{F}^-$, respectively. Again the hydrogen-bond limit seems appropriate.

Another quantity that indicates a simple hydrogen bond in $\text{H}_3\text{N}\cdots\text{HX}$ is the ^{14}N nuclear quadrupole coupling constant which has the values^{3, 20-22} $\chi(^{14}\text{N}) = -3.283 \text{ MHz}$ for $\text{X} = \text{F},$

Table 5 Comparison of halogen nuclear quadrupole coupling constants $\chi(\text{X})$ and intermolecular stretching force constants k_σ for heterodimers $\text{H}_3\text{N}\cdots\text{HX}$ with those of model systems

Molecule	³⁵ Cl		⁸¹ Br		¹²⁷ I	
	$\chi(\text{X})/\text{MHz}$	k_σ/Nm^{-1}	$\chi(\text{X})/\text{MHz}$	k_σ/Nm^{-1}	$\chi(\text{X})/\text{MHz}$	k_σ/Nm^{-1}
HX	-67 6189 ^a	—	444 681 ^d	—	-1823 4 ^c	—
$\text{HC}^{14}\text{N}\cdots\text{HX}$	-53 720 ^d	9 12 ^d	356 232(9) ^e	8 1 ^e	-1475 7(1) ^f	4 561(2) ^f
$\text{H}_3^{14}\text{N}\cdots\text{HX}$	-47 607(9) ^g	17 6(3) ^g	301 777 ^h	13 4(3) ^h	-1324 891 ⁱ	7 18(9) ⁱ
$\text{Na}^+\cdots\text{X}^-$	-5 643(4)	108 6 ^k	48 508 ^l	93 7 ^m	-262 14 ⁿ	77 0 ^m

^a Ref 10. ^b O B Dabbousi, W L Meerts, F H Deleuw and A Dymanus *Chem Phys*, 1973, 2, 473. ^c F C DeLucia, P Helming and W Gordy *Phys Rev A*, 1971, 3, 1849. ^d See footnote a of Table 1. ^e E J Campbell, A C Legon and W H Flygare *J Chem Phys*, 1983, 78, 3494 and Ref 11. ^f P W Fowler, A C Legon, and S Peebles, unpublished observations. ^g Ref 3. ^h Ref 20. ⁱ Ref 21. ^j See footnote c of Table 1. ^k See footnote b of Table 1. ^l J Cederberg, D Nitz, A Kolan, T Rasmussen, K Hoffman and S Tufte, Symposium on Molecular Structure and Spectroscopy, Ohio, 1985, Abstract MF6. ^m Calculated using $\omega_e = (2\pi c)^{-1}(k/\mu)^{\frac{1}{2}}$ from J R Rusk and W Gordy *Phys Rev A*, 1962, 127, 817. ⁿ C E Miller and J C Zorn *J Chem Phys*, 1969, 50, 3748.

– 3.248(14) MHz for X = Cl, – 3.188(8) MHz for X = Br, and – 3.182(8) MHz for X = I. The constancy of these values and their small reduction in magnitude from the free NH₃ value $\chi_0(^{14}\text{N}) = -4.090$ MHz points to a similar type of interaction in all three heterodimers involving only a weak perturbation of the electric field gradient at ¹⁴N in NH₃.

Recent *ab initio* calculations predict a simple hydrogen-bonded rather than an ion-pair form for H₃N···HCl and H₃N···HBr. Latajka *et al.*²⁴ find a long shallow minimum linking the ion-pair and hydrogen-bond forms H₃NH⁺···I⁻ and H₃N···HI, both of which have similar energy. It is of interest to note that so far only $J + 1 \leftarrow J$, $K = 0$ transitions have been fitted²¹ in the rotational spectrum of H₃N···HI, with the $K = 1$ set oddly behaved. The odd behaviour could arise from the effect of a second minimum.

4.2 The Series (CH₃)_{3-n}H_nN···HCl ($n = 3, 2$, and 0)

The experimentally determined quantities $\chi(^{35}\text{Cl})$ and k_σ for each member of the series (CH₃)_{3-n}H_nN···HCl ($n = 3, 2, 0$) are compared in Table 6.^{3,15,25} Also included are the corresponding quantities for the limiting hydrogen-bonded model HCN···HCl and the limiting ion-pair model Na⁺···Cl⁻.

Table 6 Comparison of Cl nuclear quadrupole coupling constants $\chi(^{35}\text{Cl})$ and intermolecular stretching force constants k_σ for [(CH₃)_{3-n}H_nN, HCl] with those of model systems

Molecule	$\chi(^{35}\text{Cl})/\text{MHz}$	k_σ/Nm^{-1}
HCl	-67.6189 ^a	—
HCN···HCl	-53.720 ^b	9.12 ^b
H ₃ ¹⁴ N···HCl	-47.607(9) ^c	17.6(3) ^c
CH ₃ NH ₂ ···HCl	-37.89(1) ^d	—
(CH ₃) ₃ N···HCl	-21.625(5) ^e	84(3) ^e
Na ⁺ ···Cl ⁻	-5.643(4) ^f	108.6 ^g

^a Ref. 10. ^b See footnote a of Table 1. ^c Ref. 3. ^d Ref. 25. ^e Ref. 15. ^f See footnote c of Table 1. ^g See footnote b of Table 1.

The $\chi(^{35}\text{Cl})$ values in Table 6 exhibit clearly a stepwise decrease in magnitude as NH₃ is progressively methylated, with an approximate decrement of 9 MHz per methyl group. There is a corresponding increase in k_σ , although no value of this quantity is available from the appropriate centrifugal distortion constant of CH₃NH₂···HCl because the dimer does not have axial symmetry.²⁵ Both trends are consistent with an increase in the extent of proton transfer from HCl to (CH₃)_{3-n}H_nN as n decreases. For $n = 0$, (CH₃)₃N···HCl, both $\chi(^{35}\text{Cl})$ and k_σ approach the values expected in the ion-pair limit, *i.e.* the Na⁺···Cl⁻ values. Indeed, k_σ is so large in this case that the question of the validity of its determination from D_J using equation 1 must be kept in mind. A detailed analysis, reproduced elsewhere,²⁶ predicts values of $\chi_e(^{35}\text{Cl}) = -47.7$ MHz and $k_\sigma \approx 20$ Nm⁻¹ for the hydrogen-bonded model (CH₃)₃N···HCl. The latter is four times smaller than the observed value and was obtained by extrapolating the k_σ versus N line for B···HCl in Figure 3 to the N value for trimethylamine. Clearly, the ion-pair description (CH₃)_{3-n}H_nNH⁺···Cl⁻ is more appropriate. However, an attempt to calculate $\chi_e(^{35}\text{Cl})$ by starting from the ion-pair model (CH₃)₃NH⁺···Cl⁻ and using the charge distribution of (CH₃)₃NH⁺ and the response tensors of Cl⁻ ran into convergence problems.²⁶ Hence, no quantitative conclusion about the relative contributions of (CH₃)₃N···HCl and (CH₃)₃NH⁺···Cl⁻ to a valence bond description of the molecule is yet available. Nevertheless the conclusion of this section is clear: progressive methylation of H₃N···HCl leads in the limit to a heterodimer for which the simple hydrogen-bond description alone is apparently inadequate and for which a substantial contribution from (CH₃)₃NH⁺···Cl⁻ must be invoked.

4.3 The Series (CH₃)₃N···HX (X = F, Cl, Br, I)

The conclusion of Section 4.2 encourages us to examine the series of trimethylammonium halides shown in the extreme right hand column of Figure 5. Of the generalized heterodimers (CH₃)_{3-n}H_nN···HX, the series with $n = 0$ is one in which the proton affinity of the fully methylated base is maintained at the maximum value while the proton affinity of X⁻ decreases in the order F > Cl > Br > I. Of the systems considered in this article, the propensity to form an ion pair (CH₃)_{3-n}H_nNH⁺···X⁻ should therefore be greatest for $n = 0$ and X = I. The important spectroscopic constants for the symmetric-top species $n = 0$, X = Cl, Br, and I are collected in Table 7.^{4,13-15,27} Included for comparison are those for the limiting hydrogen-bond and ion-pair models (HCN···HX and Na⁺···X⁻, respectively) and the series H₃N···HX.

We consider first and separately the dimer (CH₃)₃N···HF as a limiting example of a hydrogen-bonded complex where the base is very strong but negligible proton transfer occurs. It has been possible in this case to determine the position of the hydrogen bond proton precisely.¹³ This is available from the H,F spin-spin coupling constant D_{aa}^{HF} of (CH₃)₃¹⁵N···HF which has been measured. The separation r of the H and F nuclei in the heterodimer is related to D_{aa}^{HF} through the expression.

$$D_{aa}^{\text{HF}} \propto \langle r^{-3} \rangle \langle P_2(\cos\theta) \rangle \quad (8)$$

where the constant of proportionality involves the H and F nuclear magnetic moments and various universal constants and the term $\langle P_2(\cos\theta) \rangle = \frac{1}{2} \langle 3\cos^2\theta - 1 \rangle$ accounts for the angular oscillation of the HF subunit as defined in Figure 4. In the term $\langle r^{-3} \rangle$, the average is over the HF stretching motion but with respect to the changed equilibrium length in the complex. Equation 8 therefore allows the definition $r_0 + \delta r = \langle r^{-3} \rangle^{-\frac{1}{3}}$ of an operational HF bond length in the dimer. Clearly, the free HF bond length $r_0 = \langle r^{-3} \rangle^{-\frac{1}{3}}$ can be similarly defined and is available from the known spin-spin coupling constant D_{aa}^{HF} . The result thereby obtained¹³ for δr in (CH₃)₃N···HF is 0.041(11) Å. The value of $\theta_{\text{av}} = \cos^{-1} \langle \cos^2\theta \rangle^{\frac{1}{2}}$ used to extract $r_0 + \delta r$ from equation 8 is 14(1)^o and is discussed in detail elsewhere.¹³ Even for this very strong hydrogen-bonded system ($k_\sigma = 38.6$ Nm⁻¹), we conclude that there is only a small lengthening (~5% of the equilibrium value) of the HF bond when incorporated in the dimer. This is perhaps not unexpected since the HF bond is the most difficult to extend ($k_e = 966$ Nm⁻¹) of all single bonds.

The discussion of Section 4.2 has already dealt with the second member of the series, namely (CH₃)₃N···HCl. Unlike the HF analogue, there is evidence of an appreciable extent of proton transfer as a result of weakening the HX bond. An examination of both the $\chi(\text{X})$ and the k_σ values in Table 7 reveals that a further weakening of HX increases this effect from X = Cl through X = Br to X = I. In fact, it is of interest to estimate crudely the fractional extent of proton transfer brought about by the complete methylation of H₃N···HX to give (CH₃)₃N···HX. This can be measured by

$$f = \frac{|\chi(\text{A})| - |\chi(\text{T})|}{|\chi(\text{A})| - |\chi(\text{IP})|} \quad (9)$$

where $\chi(\text{A})$ is the halogen nuclear quadrupole coupling constant of the ammonium halide, $\chi(\text{T})$ refers to the trimethylammonium halide, and $\chi(\text{IP})$ to the model ion pair Na⁺···X⁻. This formula assumes no proton transfer for the ammonium halide. The results calculated from Table 7 are $f = 0.62, 0.80$, and 0.93 for (CH₃)₃N···HX, X = Cl, Br, and I, respectively.

The above result is confirmed when the ¹⁴N nuclear quadrupole coupling constants of the two series H₃N···HX and (CH₃)₃N···HX (X = F, Cl, Br, I) recorded in Table 8 are considered. Qualitatively, $\chi(^{14}\text{N})$ is effectively constant along the H₃N···HX series while its magnitude decreases by one half along the (CH₃)₃N···HX series. Unfortunately, $\chi(^{14}\text{N})$ for the trimethylammonium ion is not experimentally available but clearly -2.45 MHz is an upper limit to this quantity if

Table 7 Comparison of halogen nuclear quadrupole coupling constants $\chi(X)$ and intermolecular stretching force constants k_o for $[(CH_3)_3N, HX]$ with those of model systems^a

Molecule	³⁵ Cl		⁸¹ Br		¹²⁷ I	
	$\chi(X)/\text{MHz}$	k_o/Nm^{-1}	$\chi(X)/\text{MHz}$	k_o/Nm^{-1}	$\chi(X)/\text{MHz}$	k_o/Nm^{-1}
HCN...HX	- 53 720	9 12	356 232(9)	8 1	- 1475 7(1)	4 561(2)
H ₃ ¹⁴ N...HX	- 47 607(9)	17 6(3)	301 777	13 4(3)	- 1324 891(8)	7 18(9)
(CH ₃) ₃ ¹⁴ N...HX	- 21 625(5) ^b	84 (3) ^b	99 645(7) ^c	82(3) ^c	- 341 204(14) ^d	66 5(2) ^d
Na ⁺ ...X	- 5 643(4)	108 6	48 508	93 7	- 262 14	77 0

^a Values for HCN HX H₃N HX and Na⁺ X taken from Table 5 ^b Ref 15 ^c Ref 4 ^d Ref 27

Table 8 A comparison of $\chi(^{14}\text{N})/\text{MHz}$ among the ammonium and trimethylammonium halides

	H ₃ N...HX	(CH ₃) ₃ N...HX
Free base	- 4 090 ^a	- 5 502(3) ^b
X = F	- 3 283 ^c	- 4 764(3) ^d
Cl	- 3 248(14) ^e	- 3 504(5) ^f
Br	- 3 188(8) ^g	- 2 883(7) ^h
I	- 3 182(8) ^g	- 2 451(8) ^g

^a M D Marshall and J S Muentner *J Mol Spectrosc*, 1971 **39**, 94 ^b C A Rego R C Batten, and A C Legon *J Chem Phys* 1988 **89**, 696 ^c Ref 22 ^d Ref 14 ^e Ref 3 ^f Ref 15 ^g Ref 20 ^h Ref 4 ⁱ Ref 21 ^j Ref 27

Table 9 Comparison of the distances $r(\text{N}\cdots\text{X})$ in the series $(\text{CH}_3)_3\text{N}\cdots\text{HX}$ and $\text{H}_3\text{N}\cdots\text{HX}$

X	H ₃ N...HX		(CH ₃) ₃ N...HX	
	$r(\text{N}\cdots\text{X})/\text{\AA}$	Model ^a	$r(\text{N}\cdots\text{X})/\text{\AA}$	Model ^a
F	2 71 ^b	HB	2 5863(6) ^c	HB
Cl	3 137 ^d	HB	2 8164(3) ^e	HB
Br	3 255 ^f	HB	2 9607 ^g	HB
I	3 584 ^h	HB	2 9594 ^g	IP
			3 190(2) ⁱ	HB
			3 190(3) ^j	IP

^a HB = hydrogen bond model IP = ion pair model See text for discussion ^b Ref 22 ^c Ref 14 ^d Ref 3 ^e Ref 15 ^f Ref 20 ^g Ref 4 ^h Calculated from data in Ref 21 ⁱ Ref 27

$(\text{CH}_3)_3\text{N}\cdots\text{HI}$ is assumed to be wholly an ion pair. If so, and if $(\text{CH}_3)_3\text{N}\cdots\text{HF}$ can be taken as the hydrogen-bond limit, then the fractional ionic character can also be defined by

$$f = \frac{\chi(\text{HB}) - \chi(\text{obs})}{\chi(\text{HB}) - \chi(\text{IP})} \quad (10)$$

The results are 0.54, 0.82, and 1.00 for $(\text{CH}_3)_3\text{N}\cdots\text{HX}$, X = Cl, Br, and I, respectively. This approach is obviously crude but the agreement with the values determined from the halogen coupling constants is acceptable.

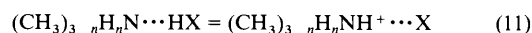
It is of interest to compare the distances $r(\text{N}\cdots\text{X})$ in the two series $\text{H}_3\text{N}\cdots\text{HX}$ and $(\text{CH}_3)_3\text{N}\cdots\text{HX}$. There is, however, a difficulty in applying the model of Section 3.3 and equation 7 to $(\text{CH}_3)_3\text{N}\cdots\text{HBr}$ and $(\text{CH}_3)_3\text{N}\cdots\text{HI}$ in which there is a preponderant contribution of the ion-pair valence bond structure to the description of the heterodimer. Briefly, this lies in the structure of the ion $(\text{CH}_3)_3\text{NH}^+$, which is assumed unchanged on dimer formation. An experimental geometry for free $(\text{CH}_3)_3\text{NH}^+$ is not available and this has been modelled by taking that of $(\text{CH}_3)_3\text{N}$ but with a proton added at a distance of 1.03 Å from N along the C₃ axis. In applying equation 7, the oscillation angle $\beta_{\text{av}} = \cos^{-1} \langle \cos^2 \beta \rangle^{1/2}$ (see Figure 4 for definition) is clearly zero for X⁻, as is I_b , in the ion-pair limit. Arguments given elsewhere lead to the assumption of $\alpha_{\text{av}} = \cos^{-1} \langle \cos^2 \alpha \rangle^{1/2} \approx 10(2)^\circ$ for the oscillation of the $(\text{CH}_3)_3\text{NH}^+$ subunit.⁴ The heterodimers $(\text{CH}_3)_3\text{N}\cdots\text{HX}$, X = F and Cl, and all of the $\text{H}_3\text{N}\cdots\text{HX}$ have been analysed using the hydrogen-bond model, the detailed assumptions about α_{av} and β_{av} in each case being given in the relevant reference. In fact the results for $r(\text{N}\cdots\text{X})$, which are listed in Table 9, are not sensitive to which model is used when the above set of assumptions is made, as may be seen in $(\text{CH}_3)_3\text{N}\cdots\text{HBr}$ and $(\text{CH}_3)_3\text{N}\cdots\text{HI}$ for which the results for both limits are given. It is clear from Table 9 that there is a general shortening of $r(\text{N}\cdots\text{X})$ when NH₃ becomes fully methylated.

5 Are the Conclusions for $(\text{CH}_3)_{3-n}\text{H}_n\text{N}\cdots\text{HX}$ Consistent with Simple Energetic Considerations?

Arguments above based on $\chi(X)$, $\chi(^{14}\text{N})$, and k_o for the series $(\text{CH}_3)_{3-n}\text{H}_n\text{N}\cdots\text{HX}$ indicate that progressive methylation of

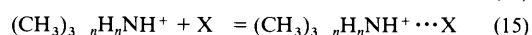
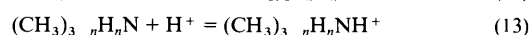
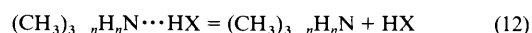
NH₃ coupled with the progressive weakening of the HX bond with respect to the process $\text{HX} = \text{H}^+ + \text{X}^-$ eventually leads to an ion pair in the gas phase when $n = 0$ and X = Br or I. In the series when $n = 0$, X = F remains a simple hydrogen-bonded dimer while X = Cl is of the intermediate type. The series $\text{H}_3\text{N}\cdots\text{HX}$ appears to exhibit no appreciable extent of proton transfer for any X. Are these conclusions consistent with simple energetics?

To answer this question, we shall examine the energy of the general process



in which a proton is transferred from HX to the base in the isolated hydrogen-bonded dimer to give the isolated ion pair. For simplicity, we shall assume that no significant change in the positions of other nuclei accompanies reaction 11. Is ΔE_{11} negative for $n = 0$, X = Br and I, and positive in other cases?

To find ΔE_{11} , we note that reaction 11 can be written as the sum of the following



The required energy change is then $\Delta E_{11} = \sum_{i=1}^5 \Delta E_i$. Values of the various ΔE_i are listed in Table 10 and have been obtained as follows.

ΔE_{13} is the negative of the gas-phase proton affinity of the base $(\text{CH}_3)_3\text{-}_n\text{H}_n\text{N}$ and values are readily available.²⁸ ΔE_{14} is given by the sum of the ionization potential of the H atom and the zero-point dissociation energy of HX minus the electron affinity of X, all of which are well known. ΔE_{15} is the electrostatic energy gained when the ions $(\text{CH}_3)_3\text{-}_n\text{H}_n\text{NH}^+$ and X⁻ are brought to the appropriate distance $r(\text{N}\cdots\text{X})$ from infinite separation. It is assumed in calculating ΔE_{15} that the cationic charge is located on N, that the repulsive contribution is negligible, and that any additional hydrogen-bond interaction $\text{N}^+ - \text{H}\cdots\text{X}$ is sufficiently independent of X to allow its neglect when comparing relative magnitudes of ΔE_{11} . The values of $r(\text{N}\cdots\text{X})$ used are those given in Table 9. The final

Table 10 Estimates of ΔE_{11} for the reaction $(\text{CH}_3)_{3-n}\text{H}_n\text{N}\cdots\text{HX} = (\text{CH}_3)_{3-n}\text{H}_n\text{NH}^+\cdots\text{X}^-$, when $n = 3$ and 0

X	$\Delta E_i/\text{kJ mol}^{-1}$				
	$i = 12^a$	$i = 13^b$	$i = 14^c$	$i = 15^d$	$i = 11^e$
$n = 3$					
F	78	-858	1554	-513	261
Cl	42	-858	1391	-443	132
Br	32	-858	1350	-427	97
I	17	-858	1312	-388	83
$n = 0$					
F	117	-946	1554	-537	188
Cl	55	-946	1391	-493	7
Br	49	-946	1350	-469	-16
I	37	-946	1312	-436	-33

See text for method of estimating ΔE_{12} the hydrogen bond dissociation energy ^b ΔE_{13} is the negative of the gas-phase proton affinity of the base and values are taken from Ref 28 but are scaled to the value recommended for NH_3 by C R Moylan and J I Brauman *Annu Rev Phys Chem* 1983 **34** 187

ΔE_{14} is the dissociation energy for $\text{HX} = \text{H}^+ + \text{X}^-$ It is the sum of the ionization potential of H and the zero point dissociation energy for $\text{HX} = \text{H} + \text{X}$ minus the electron affinity of X Values from P W Atkins

Physical Chemistry Fourth Edition Oxford University Press Oxford 1990

Coulombic energy of the ion pair $(\text{CH}_3)_3\text{H}_n\text{NH}^+\cdots\text{X}^-$ when the positive charge is assumed to reside on the N atom ^c $\Delta E_{11} = \Sigma_{12}^{15} \Delta E$ (see text)

quantity ΔE_{12} is the hydrogen-bond dissociation energy and is not experimentally available Latajka *et al*¹⁹ have calculated ΔE_{12} *ab initio* for the hydrogen-bonded models $\text{H}_3\text{N}\cdots\text{HCl}$ and $(\text{CH}_3)_3\text{N}\cdots\text{HCl}$ For the remainder of the dimers in Table 10, ΔE_{12} has been estimated from these values by assuming that it is proportional to k_σ , which is another measure of the strength of the hydrogen bond There is some evidence to support this assumption²⁹ The k_σ for $n = 0$, X = Br and I (which have significant ion-pair character) were estimated in the hydrogen bond limit using $N = 15.4$ for $(\text{CH}_3)_3\text{N}$ from reference 13 and the appropriate E values for HX (10, 5.0, 4.25, and 3.2 for X = F, Cl, Br, and I)¹¹ in equation 4 The relative errors incurred in this approximate procedure are not large and in any case ΔE_{12} makes the smallest contribution to ΔE_{11}

Table 10 shows clearly that ΔE_{11} for the proton transfer process is large and positive for all $\text{H}_3\text{N}\cdots\text{HX}$, in agreement with our conclusion that all are simple hydrogen-bonded dimers On the other hand, for the series $(\text{CH}_3)_3\text{N}\cdots\text{HX}$ (X = F, Cl, Br, I), ΔE_{11} becomes progressively smaller and changes in sign between X = Cl and X = Br This pattern is in good qualitative agreement with the experimental conclusion described above, namely that for X = F the heterodimer contains a simple hydrogen bond, X = Cl is of intermediate character while for X = Br and I the ion-pair description is more appropriate

6 What Happens when P Replaces N in $[(\text{CH}_3)_{3-n}\text{H}_n\text{N}, \text{HX}]?$

The phosphorus analogues of the ammonium and methylammonium halides are well known The solid phases of the

phosphonium halides consist of ions but in the vapour they are described as being completely dissociated into PH_3 and HX Presumably, the same is true of the trimethylphosphonium halides, for example, and in the context of the discussion here a question of interest is How do the heterodimers $[\text{H}_3\text{P}, \text{HX}]$ and $[(\text{CH}_3)_3\text{P}, \text{HX}]$ differ from their nitrogen analogues in the vapour phase? Several members of these two P-containing series have been investigated^{5, 30-34} through their rotational spectra in the manner described in Section 2.2 The aim was to determine the halogen nuclear quadrupole coupling constants $\chi(\text{X})$ and the intermolecular stretching force constants k_σ and use them as criteria of the nature of the interaction The experimental quantities are summarized in Table 11

It is immediately evident from Table 11 that heterodimers in the vapour phase of each of the phosphonium halides are of the simple hydrogen-bonded type $\text{H}_3\text{P}\cdots\text{HX}$, the order of the nuclei having been established through isotopic substitution Thus, we note that the $\chi(\text{X})$ are very similar in sign and magnitude to those of the corresponding ammonium halides and the simple model dimers $\text{HCN}\cdots\text{HX}$ (see Tables 5 and 11) The k_σ are also of the magnitude ($\sim 3-10 \text{ Nm}^{-1}$) expected for a simple hydrogen-bonded species but are much smaller than observed for the ion-pair limiting cases (compare Tables 7 and 11) Indeed by assigning a nucleophilicity $N = 4.4$ to PH_3 , it is possible to use the established electrophilicities $E = 10.0, 5.0, 4.25$, and 3.2 for HX (X = F, Cl, Br, and I, respectively) in equation 4 to predict^{11, 33} satisfactorily the observed k_σ for each $\text{H}_3\text{P}\cdots\text{HX}$ Table 11 also allows the conclusion, by similar arguments, that $(\text{CH}_3)_3\text{P}\cdots\text{HX}$ (X = Cl and Br) are of the simple hydrogen-bonded type^{5, 34}

The experimentally established conclusions for the P analogues of the ammonium and trimethylammonium halides are reinforced when the simple energetic arguments of Section 5 are applied Table 12 displays ΔE_{11} for each of the P-containing series The value of ΔE_{12} in each case has been taken from the *ab*

Table 12 Estimates of ΔE_{11} for the reaction $(\text{CH}_3)_{3-n}\text{H}_n\text{P}\cdots\text{HX} = (\text{CH}_3)_{3-n}\text{H}_n\text{PH}^+\cdots\text{X}^-$, when $n = 3$ and 0

X	$\Delta E_i/\text{kJ mol}^{-1a}$				
	$i = 12$	$i = 13$	$i = 14$	$i = 15$	$i = 11$
$n = 3$					
F	26	-795	1554	-420	365
Cl	14	-795	1391	-358	252
Br	12	-795	1350	-343	224
I	8	-795	1312	-317	208
$n = 0$					
F ^b	—	—	—	—	—
Cl	25	-948	1391	-385 ^c	83
Br	19 ^d	-948	1350	-370 ^c	51
I	12 ^d	-948	1312	-347 ^c	29

^a See footnotes to Table 10 for the definition of the various ΔE_i ^b No estimates of ΔE_{12} and $r(\text{P}\cdots\text{F})$ in $(\text{CH}_3)_3\text{P}\cdots\text{HF}$ are available ^c Calculated from experimental $r(\text{P}\cdots\text{X})$ in Refs 5 and 34 ^d Ref 35 ^e Calculated from the *ab initio* $r(\text{P}\cdots\text{X})$ in Ref 35

Table 11 Comparison of halogen nuclear quadrupole coupling constants $\chi(\text{X})$ and intermolecular stretching force constants k_σ for $[\text{PH}_3, \text{HX}]$ and $[(\text{CH}_3)_3\text{P}, \text{HX}]$ with those of model systems^a

Molecule	³⁵ Cl		⁸¹ Br		¹²⁷ I	
	$\chi(\text{X})/\text{MHz}$	k_σ/Nm^{-1}	$\chi(\text{X})/\text{MHz}$	k_σ/Nm^{-1}	$\chi(\text{X})/\text{MHz}$	k_σ/Nm^{-1}
$\text{HCN}\cdots\text{HX}$	-53.270	9.12	356.232(9)	8.1	-1475.7(1)	4.561(2)
$\text{H}_3\text{P}\cdots\text{HX}$	-53.861(3) ^b	5.9 ^b	357.521(6) ^c	4.3 ^c	-1461.022(8) ^d	3.409(2) ^d
$(\text{CH}_3)_3\text{P}\cdots\text{HX}$	-50.486(7) ^e	10.48(7) ^e	322.99(4) ^f	8.28(4) ^f	—	—
$\text{Na}^+\cdots\text{X}$	-5.643(4)	108.6	48.508	93.7	-262.14	77.0

Values for HCN, HX and $\text{Na}^+\cdots\text{X}$ taken from Table 5 ^b A C Legon and L C Willoughby unpublished observations Ref 32 and Ref 11 ^d Ref 33 Ref 5 Ref 34

ab initio calculations of Muller and Reinhold³⁵ The gas-phase proton affinities ($-\Delta E_{13}$) of PH_3 and $(\text{CH}_3)_3\text{P}$ are experimentally available²⁸ while the required ΔE_{14} values are transferred from Table 10 Each ΔE_{15} has been estimated as described in Section 5 using the $r(\text{P}\cdots\text{X})$ taken from references 5,30–35, as appropriate It is clear from Table 12 that ΔE_{11} is large and positive in each heterodimer, thereby establishing that the simple hydrogen-bonded structure $(\text{CH}_3)_{3-n}\text{H}_n\text{P}\cdots\text{HX}$ ($n = 0$ and 3) is favoured energetically relative to the corresponding ion pair $(\text{CH}_3)_{3-n}\text{H}_n\text{PH}^+\cdots\text{X}^-$

Why is it that $(\text{CH}_3)_3\text{P}\cdots\text{HX}$ are not ion-pair heterodimers in the gas phase while $(\text{CH}_3)_3\text{N}\cdots\text{HX}$ ($\text{X} = \text{Br}$ and I) are, given that the gas-phase proton affinities ($-\Delta E_{13}$) of $(\text{CH}_3)_3\text{N}$ and $(\text{CH}_3)_3\text{P}$ are identical²⁸ within experimental error? The answer is clear and lies in the relative magnitude of ΔE_{15} in the two series Obviously, $r(\text{P}\cdots\text{X})$ is greater than $r(\text{N}\cdots\text{X})$ for a given X and hence ΔE_{15} is more negative in the nitrogen analogue Since for a given X the difference in ΔE_{12} is small and the ΔE_{14} are identical, the predominant term in stabilizing the ion-pair form in the N series is ΔE_{15} This is of sufficient magnitude to make ΔE_{11} negative for the trimethylammonium halides ($\text{X} = \text{Br}$ and I) but not in the case of any of the trimethylphosphonium halides In short, the large P atom ensures that ΔE_{15} is insufficiently negative in the latter group

7 Conclusions

The spectroscopic constants of the series of dimers $(\text{CH}_3)_{3-n}\text{H}_n\text{N}\cdots\text{HX}$ and their phosphorus analogues, obtained from rotational spectroscopy conducted on supersonically expanded jets of appropriate gas mixtures in argon, allow the conclusion that the species $\text{H}_3\text{N}\cdots\text{HX}$ and $\text{H}_3\text{P}\cdots\text{HX}$ can all be described as the simple hydrogen-bonded type, without the need to invoke an appreciable extent of proton transfer However, along the series $(\text{CH}_3)_3\text{N}\cdots\text{HX}$, where $\text{X} = \text{F}$, Cl , Br , and I , the progressive weakening of the HX bond with respect to the dissociation products H^+ and X^- favours the ion-pair Experiment shows that for $\text{X} = \text{Br}$ and I , the ion-pair form is the preponderant contribution to a simple valence-bond description of the molecule Across the series $(\text{CH}_3)_{3-n}\text{H}_n\text{N}\cdots\text{HCl}$, where $n = 3, 2$, and 0 , the progressive methylation of NH_3 increases its gas-phase proton affinity so that the extent of proton transfer becomes appreciable for $(\text{CH}_3)_3\text{N}\cdots\text{HCl}$ The series $(\text{CH}_3)_3\text{P}\cdots\text{HX}$, where $\text{X} = \text{Cl}$ and Br , appears to behave differently, with the simple hydrogen-bond model appropriate in both cases This behaviour contrasts with the observations for $(\text{CH}_3)_3\text{N}\cdots\text{HX}$, where $\text{X} = \text{Cl}$ and Br , and the difference is attributed to the decrease of Coulombic attraction in the gas-phase ion pair of the phosphorus compounds because of the larger radius of P than N

These conclusions are broadly in agreement with a number of the more recent *ab initio* calculations^{19, 24, 35} which indicate ion-pair forms for $(\text{CH}_3)_3\text{N}\cdots\text{HX}$, where $\text{X} = \text{Cl}$, Br , and I , but simple hydrogen-bonded structures for all other species discussed in this article These *ab initio* calculations also tend to find only a single minimum in the potential energy surface, rather than one associated with the hydrogen-bonded form and another associated with the ion-pair form This is physically reasonable, for the distance that the hydrogen-bond proton needs to move to yield the ion-pair form is only $\approx 0.5 \text{ \AA}$ in most cases This would imply a very sharp, almost singular potential energy barrier between the two forms

So it is that the natures of the heterodimers in the vapour above the various ammonium halides $[(\text{CH}_3)_{3-n}\text{H}_n\text{N}, \text{HX}]$ and phosphonium halides $[(\text{CH}_3)_{3-n}\text{H}_n\text{P}, \text{HX}]$ have been established by experiment and theory Ammonium chloride itself holds a special position in these series as one of the archetypal donor-acceptor systems and consequently there is a history associated with attempts to characterize the interaction The author's speculations in the Introduction are by no means the first

For example, Mulliken³⁶ alluded to inner complexes $\text{H}_3\text{NH}^+\cdots\text{Cl}^-$ and outer complexes $\text{H}_3\text{N}\cdots\text{HCl}$ in his classic

paper on electron donors and acceptors in 1952 but at that time there had been no experimental characterization of the heterodimer He returned to the theme in his Nobel Prize lecture³⁷ in 1966, in which he devoted some time to a discussion of the then unpublished but later famous early *ab initio* calculations by Clementi^{38–40} These calculations were the first to provide a detailed description of the charge redistribution that occurs in the process of proton transfer and, although it now appears that they found an equilibrium geometry with too much ion-pair character for the $(\text{NH}_3, \text{HCl})$ system, Mulliken's comments³⁶ on them are worth quoting, for presumably they are appropriate to cases such as $(\text{CH}_3)_3\text{N}\cdots\text{HX}$ ($\text{X} = \text{Cl}$, Br and I) "Clementi's calculations show a gradual transfer of charge from the NH_3 to the Cl atom, accompanied by some stretching of the $\text{H}-\text{Cl}$ distance, until at equilibrium a structure approaching that of an NH_4^+Cl^- ion pair, but with considerable polarization of the Cl^- (H -bonding of NH_4^+ to Cl^-) is attained The $\text{NH}_3 + \text{HCl}$ system is thus apparently an example of ion-pair formation rather than ordinary loose hydrogen bonding, however, the changes in charge distribution during the early stages of approach of the HCl and NH_3 should probably be similar to those in ordinary H -bonding and thus instructive for the latter "

Clementi's calculations and Mulliken's comments stimulated new experimental attempts to characterize the heterodimer in ammonium chloride vapour (through mass spectrometry⁴¹ and electron diffraction⁴²) These were followed by larger and more refined *ab initio* calculations Raffanetti and Phillips,⁴³ Latajka *et al.*,¹⁹ and Brčić *et al.*⁴⁴, for example, showed conclusively that the equilibrium form of the dimer is $\text{H}_3\text{N}\cdots\text{HCl}$ with no second minimum corresponding to $\text{H}_3\text{NH}^+\cdots\text{Cl}^-$, in agreement with the experimental result discussed above

Finally, the infrared spectroscopy of the complexes $(\text{CH}_3)_{3-n}\text{H}_n\text{N}\cdots\text{HX}$ isolated in argon matrices at low temperature^{18, 45, 46} has identified $\text{N}\cdots\text{H}\cdots\text{X}$ antisymmetric stretching modes and allowed the existence of ion pairs $(\text{CH}_3)_{3-n}\text{H}_n\text{NH}^+\cdots\text{X}^-$ to be postulated in the cases $\text{X} = \text{Cl}$ and Br NMR spectroscopy of $(\text{CH}_3)_3\text{N}\cdots\text{Br}$ in the gas phase also indicates that this species should be classified as an ion pair⁴⁷

Acknowledgements I am pleased to have this opportunity to acknowledge the contribution of Elizabeth Goodwin, Nigel Howard, Joanna Thorn, Andrew Wallwork, and, especially, Charles Willoughby and Christopher Rego to our work on the series $(\text{CH}_3)_{3-n}\text{H}_n\text{Y}\cdots\text{HX}$ ($\text{Y} = \text{N}$ and P , $\text{X} = \text{F}$, Cl , Br , I) reviewed here

8 References

- 1 R E Smalley, L Wharton, and D H Levy, *Acc Chem Res*, 1977, **10**, 139
- 2 E J Goodwin, N W Howard, and A C Legon, *Chem Phys Lett*, 1986, **131**, 319
- 3 N W Howard and A C Legon, *J Chem Phys*, 1988, **88**, 4694
- 4 A C Legon, A L Wallwork, and C A Rego, *J Chem Phys*, 1990, **92**, 6397
- 5 A C Legon and C A Rego, *J Chem Soc Faraday Trans*, 1990, **86**, 1915
- 6 T J Balle and W H Flygare, *Rev Sci Instrum*, 1981, **52**, 33
- 7 A C Legon, *Annu Rev Phys Chem*, 1983, **34**, 275
- 8 D J Millen, *Can J Chem*, 1985, **63**, 1477
- 9 W Gordy and R L Cook, in 'Microwave Molecular Spectra', Technique of Organic Chemistry, Vol IX, ed A Weissberger, Interscience, New York, 1970, Chapter 14
- 10 E W Kaiser, *J Chem Phys*, 1970, **53**, 1686
- 11 A C Legon and D J Millen, *J Am Chem Soc*, 1987, **109**, 356
- 12 A C Legon and D J Millen, *Proc R Soc London Ser A* 1986, **404**, 89
- 13 A C Legon and C A Rego, *Chem Phys Lett*, 1989, **154**, 468
- 14 A C Legon and C A Rego, *Chem Phys Lett*, 1989, **157**, 243
- 15 A C Legon and C A Rego, *J Chem Soc Chem Commun* 1988, 1496 *J Chem Phys* 1989, **90**, 6867
- 16 J Baker, A D Buckingham, P W Fowler, P Lazzaretto, E Steiner and R Zanasi, *J Chem Soc Faraday Trans 2*, 1989, **85**, 901

- 17 P W Fowler, personal communication
- 18 A J Barnes, T R Beech, and Z Mielke, *J Chem Soc Faraday Trans 2*, 1984, **80**, 455
- 19 Z Latajka, S Sakai, K Morokuma, and H Ratajczak, *Chem Phys Lett*, 1984, **110**, 464
- 20 N W Howard and A C Legon, *J Chem Phys*, 1987, **86**, 6722
- 21 A C Legon and D Stephenson, *J Chem Soc Faraday Trans*, 1992, **88**, 761
- 22 B J Howard and P R R Langridge-Smith, personal communication of D_J and $\chi(^{14}\text{N})$ for $\text{H}_3\text{N}\cdots\text{HF}$
- 23 Calculated from $\omega_e = (2\pi c)^{-1}(k/\mu)^{1/2}$ and the value of ω_e given in S E Veazey and W Gordy, *Phys Rev A*, 1965, **138**, 1303
- 24 Z Latajka, S Scheiner, and H Ratajczak, *Chem Phys*, 1992, **166**, 85
- 25 A C Legon and C A Rego, *Chem Phys Lett*, 1989, **162**, 369
- 26 P W Fowler, A C Legon, C A Rego, and P Tole, *Chem Phys*, 1989 **134**, 297
- 27 A C Legon and C A Rego, *J Chem Phys*, in press
- 28 S Ikuta, P Kebarle, G M Bancroft, T Chan, and R J Puddephatt, *J Am Chem Soc*, 1982, **104**, 5899
- 29 A C Legon, D J Millen, and H M North, *J Chem Phys*, 1987, **86**, 2530
- 30 A C Legon and L C Willoughby, *Chem Phys*, 1983, **74**, 127
- 31 A C Legon and L C Willoughby, *J Chem Soc Chem Commun*, 1982, 997 and unpublished observations
- 32 L C Willoughby and A C Legon, *J Phys Chem*, 1983, **87**, 2085
- 33 N W Howard, A C Legon, and G J Luscombe, *J Chem Soc Faraday Trans*, 1991, **87**, 507
- 34 A C Legon and J C Thorn, unpublished observations
- 35 B Muller and J Reinhold, *Chem Phys Lett*, 1992, **196**, 363
- 36 R S Mulliken, *J Phys Chem*, 1952, **56**, 801
- 37 R S Mulliken, *Science*, 1967, **157**, 13
- 38 E Clementi, *J Chem Phys*, 1967, **46**, 3851
- 39 E Clementi, *J Chem Phys*, 1967, **47**, 2323
- 40 E Clementi and J N Gayles, *J Chem Phys*, 1967, **47**, 3837
- 41 P Goldfinger and G Verhaegen, *J Chem Phys*, 1969, **50**, 1467
- 42 S Shibata, *Acta Chem Scand*, 1970, **24**, 705
- 43 R C Raffanetti and D H Phillips, *J Chem Phys*, 1979, **71**, 5434
- 44 A Brciz, A Karpfen, H Lischka, and P Schuster, *Chem Phys*, 1984, **89**, 337
- 45 A J Barnes, J N S Kuzniarski, and Z Mielke, *J Chem Soc Faraday Trans 2*, 1984, **80**, 465
- 46 A J Barnes and M P Wright, *J Chem Soc Faraday Trans 2*, 1986, **82**, 153
- 47 N S Golubev and G S Denisov, *Sov J Chem Phys*, 1982, **1**, 965